Acta Cryst. (1977). A33, 823–828

The Valence-Charge Density of Graphite

BY R. CHEN* AND P. TRUCANO

Department of Crystallography, University of Pittsburgh, Pittsburgh, Pennsylvania 15260, *USA*

AND R. F. STEWART

Mellon Institute, Carnegie-Mellon University, Pittsburgh, Pennsylvania 15213, *USA*

(*Received* 4 *April* 1977; *accepted* 29 *April* 1977)

A full sphere of data extending to $(\sin\theta/\lambda)=1{\cdot}2$ Å^{-1} and containing 1595 reflections was measured with small, natural, single crystals of graphite and Mo $K\alpha$ radiation. With the structure assumed to be in space group $P6_3/mmc$, the valence-charge density of the two independent C atoms was represented by a finite multipole expansion containing products of single-exponential radial functions and tesseral harmonics. A full-matrix, least-squares refinement of the model charge was computed where populations of the multipole deformations, thermal parameters, scale, and extinction parameters were refined. The experimental data fit a model charge density containing highly directional build-ups of charge to 2 e Å^{-3} between nearest neighbors in the basal plane. No structure was evident in the charge density between the basal planes. The refinable parameter, α, in the exponential radial function was $3{\cdot}16\pm0{\cdot}05$ bohr^{-1}. The charge density and associated parameters are consistent with strong covalent bonding of sp^2 character in the basal plane of graphite and minimal interactions between the layers.

Introduction

Charge-density analysis is especially productive when applied to first-row elements because the valence population represents a substantial proportion of the total number of electrons and because the theoretical calculations are more tractable for these elements. Diamond and beryllium have recently been studied by Stewart (1973, 1977) using the data of Göttlicher & Wölfel (1959) and Brown (1972) respectively. Graphite is a particularly interesting study in this sequence because the primarily sp^2 bonding between C atoms contrasts with the sp^3-like bonding in diamond. Furthermore, the site symmetry of the C atoms in graphite is identical with that of the atoms in Be. Comparisons then indicate the ability of refinement procedures to reflect the differences in charge density that are expected, since symmetry conditions alone do not ensure a difference in the natures of the charge densities.

The structure of graphite given by Bernal (1924) is shown in Fig. 1. Two independent C atoms, C(1) and C(2), form the asymmetric unit. C(1) has neighbors above and below it in adjacent layers, while C(2) is above and below the centers of the hexagonal rings in adjacent layers. Goodman (1976) found the Bernal structure applied to 'unfaulted and unstrained' regions but that strains or faults may introduce new symmetries. Proposed graphite structures with lower than hexagonal symmetry (Lukesh, 1950; Pauling, 1966; Ergun, 1973)† have been examined by Trucano & Chen (1975) using neutron diffraction. No evidence of lower symmetry was found in our crystals, and therefore it was assumed that the classical structure of graphite in space group $P6_3/mmc$ accurately reflects the structure of our samples. Following the careful collection of a large data set, charge-density refinements were carried out to characterize the valence-charge density of the two C atoms in the graphite structure.

* Present address: Department of Physics, National Taiwan Normal University, Taipei, Taiwan, 107, Republic of China.

† An error in Ergun's analysis was pointed out by Donahue (1975).

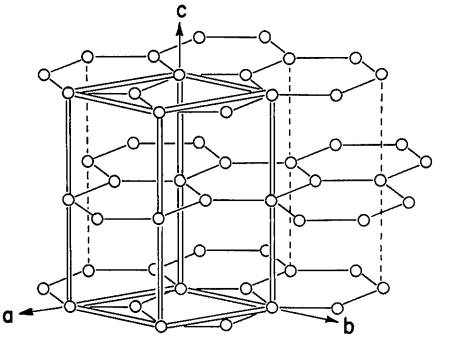

Fig. 1. The structure of graphite (Bernal, 1924). The directions of the hexagonal unit-cell vectors, **a**, **b**, and **c**, are indicated. The unit cell, outlined in double lines, contains two independent atoms, C(1) and C(2), which are related to the other two atoms in the unit cell by a center of symmetry half-way between layers and above C(1). C(1) has neighbors above and below it in adjacent layers, while C(2) is above and below the centers of the hexagonal rings in adjacent layers.

Data collection

The graphite sample was selected from a group of 30 small, natural, single crystals. Several showed good crystallinity; the crystal selected for the X-ray diffraction experiments was in the form of an irregular plate about $0{\cdot}2 \times 0{\cdot}4$ mm, and having a thickness of 0·04 mm along **c**. The crystal volume was $0{\cdot}35 \times 10^{-2}$ mm^3. The linear absorption coefficient of graphite is 1·2 cm^{-1} for Mo radiation (*International Tables for X-ray Crystallography*, 1968), which makes absorption corrections of little consequence. Nonetheless, an absorption correction was eventually made because the results were needed for secondary-extinction corrections, and in this procedure, 32 grid points and 7 boundary planes were used to describe the crystal.

Although the crystal showed unusual perfection for graphite, it was far from ideal for single-crystal data collection. The mosaic spread was nominally between 0·4 to 0·8° f.w.h.m. depending on the reflection and the orientation of the crystal when the reflection was scanned. Up to 15% of the integrated intensity of a reflection could be found outside the main peak in uneven tails which extended to 3° in θ. To obtain good agreement in the integrated intensities of symmetry-related reflections, or even the same reflection scanned at different azimuthal angles, care had to be taken to include the intensity in the tails. These conditions necessitated the use of ω scans of up to 8° with a fixed counter, set so that it would receive all wavelengths in the incident beam. No indications of multiple-reflection effects were found.

A flat pyrolitic-graphite monochromator set to diffract Mo $K\alpha$ radiation was used on a Picker FACS-I automatic diffractometer. The crystal was mounted close to the [110] direction. ω-scans were made at 1° min^{-1}, and backgrounds were counted for 10 s at the high and low-angle extremes of the scan. Three standard reflections were measured after every six reflections and were used to correct for variations in the incident beam intensity.

The orientation of the crystal was obtained by carefully hand-centering 30 reflections distributed over the diffracting sphere and the angles so determined were used to calculate the lattice parameters and the orientation matrix. Cell dimensions based on this refinement were $a = 2{\cdot}461$ (4) and $c = 6{\cdot}706$ (2) Å at 293 °K. A full sphere of data was collected to a maximum 2θ angle of 120°; 1595 different reflections were measured. Of these, 741 had integrated intensities less than 2σ, the majority of these being systematic absences for space group $P6_3/mmc$. The number of symmetry-independent reflections with integrated intensities larger than 2σ was 99. In the refinements described below the assumed standard deviations were based on counting statistics plus 0·025 of the net counts in the peak. Comparisons of symmetry-related pairs showed that this assumption was justified for higher-order reflections. However, the low-order data contained a very small error due to counting statistics and the assumed errors were thus underestimated. The use of other weighting schemes did not improve or materially change the results.

Theory

To derive the electron-charge density in crystalline graphite, an analysis of the diffraction data following that described by Stewart (1976) was used. Kinematic diffraction theory was assumed to apply to the X-ray intensities that were observed, *i.e.* after Lp corrections the intensities are set proportional to $|F|^2$, where F is the structure factor for the graphite unit cell. Corrections for absorption and extinction were subsequently made to more closely approximate this assumption and are discussed below.

The thermal motion of the C atoms was assumed to be harmonic and the charge density associated with each atom was assumed to move with the nucleus. Furthermore, it was assumed that the charge is not deformed when an atom moves, and that the total charge can be represented by a sum of charge densities centered on the nuclei. The resultant charge density then is a 'static' charge density which is a complicated average over the states assumed by the electrons as the atoms of the crystal vibrate.

The charge density associated with a particular atom was assumed to consist of an undeformed $1s^2$ shell and a deformable valence part. The cores were assumed to have a fixed population of two electrons and the valence electrons were described by a complete set of deformation functions with variable population parameters for each deformation term. The charge $\varrho_p(\mathbf{r})$ associated with a particular atom p was written as:

$$\varrho_p(\mathbf{r}) = \sum_{l=0}^{L} \left[\sum_{m=0}^{l} P^e_{p,lm} (4\pi)^{-1} R_{p,l} \mathbf{A}^m_l(\cos\theta_p) \cos m\varphi_p \right] + \left[\sum_{m=1}^{l} P^o_{p,lm} (4\pi)^{-1} R_{p,l} \mathbf{A}^m_l(\cos\theta_p) \sin m\varphi_p \right] \quad (1)$$

where $P^{e,o}_{p,lm}$ are the population coefficients of a particular deformation described by the parameters l and m; e and o indicate whether the deformation is even or odd with respect to φ. $\mathbf{A}^m_l(\cos\theta)$ are proportional to associated Legendre functions and θ and φ are polar coordinates in a local coordinate system at atom p. $R_{p,l}$ is a radial function of the form

$$R_{p,0} = (2/P_{p,0})\chi^2_{1s}(r_p) + (\alpha_p^5/4!) r_p^2 \exp(-\alpha_p r_p),$$
$$R_{p,l} = [\alpha_p^{l+3}/(l+2)!] r_p^l \exp(-\alpha_p r_p), \quad l \geq 1.$$

Other powers of r_p in $R_{p,l}$ were used in the refinements, but r_p^l gave the best fit to the data. α_p was made a refinable parameter.

The deformation terms in (1) must conform to the site symmetry of atom p. The two independent atoms in the graphite structure are each at positions with site symmetry $\bar{6}m2$. Consequently, many of the terms in (1) can be set to zero. Up to seventh order, $l = 7$, there are only eight non-zero population coefficients in (1).

These terms are listed in Table 1, along with the radial functions R_{pl} and the angular functions $A_l^m(\cos\theta)\{^{\cos m\varphi}_{\sin m\varphi}\}$.

Equation (1) was Fourier-transformed to give a structure factor for each atom; the population coefficients and radial parameters, α_p, were incorporated into a least-squares refinement. Graphite's two independent atoms call for up to eight population parameters for each atom, two thermal parameters for each atom, and a radial function parameter α_p for each atom and a scale factor, or a total of 23 parameters.

The scale factor multiplied only terms with fixed populations, such as the $1s^2$ cores, in the calculated structure factors used in the refinement. The populations quoted in Table 2, which shows the refinement results, are the $P^{o,e}_{p,lm}$ of (1) divided by the final scale factor, so that $P_{p,00}$ is a measure of the total valence charge associated with atom p, in units of electrons, e. An integration of higher-order deformations over all space yields zero so that these terms represent a redistribution of the spherical charge in the $P_{p,00}$ terms.

Refinement results

Refinements were done by systematically increasing the number of refinable parameters. After a refinement converged, a new deformation term was added and it alone varied to obtain a suitable initial value for the full-matrix least-squares refinement of all parameters. This procedure was repeated until all eight deformation terms were refined for C(1) and C(2) along with the thermal parameters, scale and the exponential term α. The results of these refinements are summarized in Table 2. The high correlation between the α_p's and the

Table 1. *Multipole radial and angular basis functions for atomic charge-density expansions*

l and m specify the order of the deformation. α is a refinable parameter in the radial term $R_l(r)$ where r is the distance from the atom center. $A_l^m(\cos\theta)\{^{\cos m\varphi}_{\sin m\varphi}\}$ are the angular functions where $A_l^m(\cos\theta)$ are proportional to associated Legendre functions. θ is measured from the c axis of the hexagonal cell and φ is measured from the a axis. Only deformations allowed by $\bar{6}m2$ symmetry are listed.

l,m	$R_l(r)$	$A_l^m(\cos\theta)\{^{\cos m\varphi}_{\sin m\varphi}\}$
0,0	$(\alpha^5/4!)r^2\exp(-\alpha r)$	1
2,0	$(\alpha^5/4!)r^2\exp(-\alpha r)$	$3\cos^2\theta-1$
3,3	$(\alpha^6/5!)r^3\exp(-\alpha r)$	$(1-\cos^2\theta)^{3/2}\sin 3\varphi$
4,0	$(\alpha^7/6!)r^4\exp(-\alpha r)$	$7\cos^4\theta-6\cos^2\theta+3/5$
5,3	$(\alpha^8/7!)r^5\exp(-\alpha r)$	$(9\cos^2\theta-1)(1-\cos^2\theta)^{3/2}\sin 3\varphi$
6,0	$(\alpha^9/8!)r^6\exp(-\alpha r)$	$11\cos^6\theta-15\cos^4\theta+5\cos^2\theta-5/21$
6,6	$(\alpha^9/8!)r^6\exp(-\alpha r)$	$(1-\cos^2\theta)^3\cos 6\varphi$
7,3	$(\alpha^{10}/9!)r^7\exp(-\alpha r)$	$(13\cos^4\theta-6\cos^2\theta+3/11)(1-\cos^2\theta)^{3/2}\sin 3\varphi$

Table 2. *Refinement results for varying increasing numbers of deformation population parameters $P_{p,lm}$*

The first subscript, p, refers to atom C(1) or C(2). Refinements in columns (1)–(5) were done without extinction corrections. The results in column (6) include refinement on extinction parameters as well as all significant deformation terms. The radial function exponent, α, and the thermal parameters, $U_{p,ii}$, are in units of bohr^{-1} and Å^2, respectively and $P_{p,00}$ is in units of electrons.

	(1) Free atom	(2) $P_{p,00}$	(3) $+P_{p,20}$ $+P_{p,00}$	(4) $P_{p,00}$ $+P_{p,20}$ $+P_{p,33}$	(5) $P_{p,00}$ $+P_{p,20}$ $+P_{p,33}$ $+P_{p,40}$	(6) Including extinction
α		3·4 (1)	3·4 (1)	3·28 (8)	3·28 (8)	3·16 (5)
$P_{1,00}$		4·3 (5)	4·3 (4)	3·5 (4)	3·4 (4)	4·3 (2)
$P_{1,20}$			−0·3 (2)	−0·13 (8)	−0·1 (1)	−0·3 (1)
$P_{1,33}$				−1·6 (3)	−1·6 (3)	−0·9 (1)
$P_{1,40}$					0·3 (3)	
$U_{1,11}$	0·0038 (5)	0·0027 (5)	0·0025 (5)	0·0030 (2)	0·0030 (3)	0·0030 (2)
$U_{1,33}$	0·0140 (9)	0·0126 (8)	0·0130 (10)	0·0137 (7)	0·0138 (7)	0·0140 (3)
$P_{2,00}$		4·2 (5)	4·2 (4)	3·4 (4)	3·4 (4)	4·3 (2)
$P_{2,20}$			−0·3 (2)	−0·1 (1)	−0·1 (1)	−0·2 (1)
$P_{2,33}$				1·7 (4)	1·7 (4)	0·8 (1)
$P_{2,40}$					0·5 (3)	
$U_{2,11}$	0·0041 (4)	0·0027 (5)	0·0026 (5)	0·0033 (2)	0·0033 (3)	0·0033 (1)
$U_{2,33}$	0·0148 (9)	0·0129 (8)	0·0132 (9)	0·0137 (7)	0·0138 (6)	0·0140 (3)
R	6·0	6·2	6·0	4·4	4·1	3·8
R_w	6·1	5·2	5·1	3·0	2·9	3·5
GOF	6·8	7·4	7·3	4·5	4·5	1·6

monopole population parameters, $P_{p,00}$, necessitated the use of only one α to describe the radial functions of C(1) and C(2). Column (1) shows the results with free-atom scattering factors, taken from *International Tables for X-ray Crystallography* (1974), assumed. Two thermal parameters for each C atom and an overall scale factor were the only refinable variables. Columns (2)–(5) show the results of progressively more general refinements. Population parameters that were less than one estimated standard deviation were omitted from the table.

The monopole populations, $P_{p,00}$, were unrealistically low after the four charge-density refinements summarized in columns (4) and (5) of Table 2. $P_{p,33}$, the octapole population, was the major factor in decreasing the refinement R factors. $P_{p,20}$ and $P_{p,40}$ were of marginal significance but were included in the table when they exceeded 1σ. The thermal parameters did not vary greatly throughout the refinement procedure.

The low sum of $P_{1,00}+P_{2,00}$, which must be eight electrons to maintain charge neutrality in the crystal, and the low observed structure factors relative to calculated structure factors on several low-order reflections, indicated that extinction was a problem. To account for these effects, the extinction formalism of Becker & Coppens (1975) for anisotropic secondary extinction, incorporated into a refinement program developed by Hansen & Coppens (1976), was used. This program is capable of refining the charge density for graphite simultaneously with anisotropic extinction parameters. Refinements were done with various extinction models. A Lorentzian mosaic distribution and constraint conditions $g_{11}=g_{22}=2g_{12}$ and $g_{23}=g_{13}=0$ gave reasonable extinction parameters and the largest improvement in R. The full sphere of data was averaged to a half sphere of 541 reflections for the calculations which included extinction parameters as refinement variables.

The results of this refinement are shown in column (6) of Table 2. Both $P_{p,00}$'s increased and α decreased slightly, as did the $P_{p,33}$'s. Most other parameters showed little change and R was substantially improved. The refined extinction parameters were $g_{11}=(0{\cdot}7\pm0{\cdot}2)\times10^{-6}$ and $g_{33}=(14\pm10)\times10^{-6}$, which correspond to mosaic spreads of 40″ and 9″ respectively. Of the 541 reflections refined in the extinction refinement, nine intensities had corrections greater than 2% and four reflections had corrections greater than 5%. The intensities of 002 and 004 had 46 and 9% corrections, respectively, and the intensities of 112 and $\bar{1}\bar{1}2$ had 10% corrections.

Correlations above 0·5 for the most general refinements, before and after extinction was included, are listed in Table 3. In the refinement without extinction, correlations between scale, α, and the two $P_{p,00}$'s ranged from 0·77 to 0·91. All other correlations were less than 0·61. When extinction was added to the refinement, these high correlations were reduced to less than 0·77.

Charge-density maps

A map of the valence-charge density was formed with the experimentally determined α and population parameters $P^{e,o}_{p,lm}$ in (1) for the charge associated with each C atom in the unit cell. The maps are not Fourier maps, and the distinctions should be kept in mind. There are no termination errors in the calculated maps and the density is a 'static' charge density because the thermal smearing has been factored out.

The charge density associated with one atom in the unit cell can extend over a rather long range depending on α and the order of the deformations. Therefore, the total charge density at any one point in the unit cell may have appreciable contributions from many atoms. To accurately construct the total charge density, a sum was made over the contributions of all atoms within

Table 3. *Correlations greater than* 0·5 *for the most general refinements before and after inclusion of extinction parameters*

$P_{p,lm}$ and $U_{p,ii}$ refer to population parameters and thermal parameters, respectively, and the first subscript, p, refers to atoms C(1) or C(2).

Before extinction corrections

	α	$P_{1,00}$	$P_{1,33}$	$U_{1,11}$	$U_{1,33}$	$P_{2,00}$	$U_{2,11}$	$U_{2,33}$
Scale	−0·77	−0·81		0·53		−0·80	0·61	
α		0·91				0·91		
$P_{1,00}$			−0·51			0·88		
$P_{2,00}$					−0·58			
$U_{1,11}$								0·55
$P_{2,20}$								−0·58

After extinction corrections

	α	$P_{1,00}$	$P_{2,00}$	$U_{1,11}$	$U_{1,33}$	$P_{2,00}$	$P_{2,33}$	$U_{2,11}$	$U_{2,33}$
Scale	−0·72			0·51				0·56	
α		−0·71				−0·71			
$P_{1,00}$			−0·56			0·77			
$P_{1,20}$					0·53				
$P_{1,33}$							−0·59		
$P_{2,20}$									−0·56

3·5 Å of the point of interest. Sections through the unit cell were made and contour plots drawn. A section was made through the basal plane of graphite, and another was made perpendicular to this plane so that it contained the line connecting C(1) and C(2). Valence-charge density maps of these two sections, derived from parameters obtained before and after extinction was included, are shown in Figs. 2 and 3.

Only the valence-electron density is plotted in Figs. 2 and 3, *i.e.* the $\varrho_{1s}(\mathbf{r})$ centered at each C atom location has been eliminated. $\varrho_{1s}(\mathbf{r})$ would be a sharply peaked radially symmetric function. The countours in the center of the hexagonal ring represent the lowest charge density of 0·2 e Å^{-3}. The density increases as the perimeter of the ring is approached. Maximum contours at 2·0 e Å^{-3} are found in the center of the covalent bonds between C atoms. The contours show decreasing density as the atomic positions are approached because of the exclusion of the $1s^2$ density.

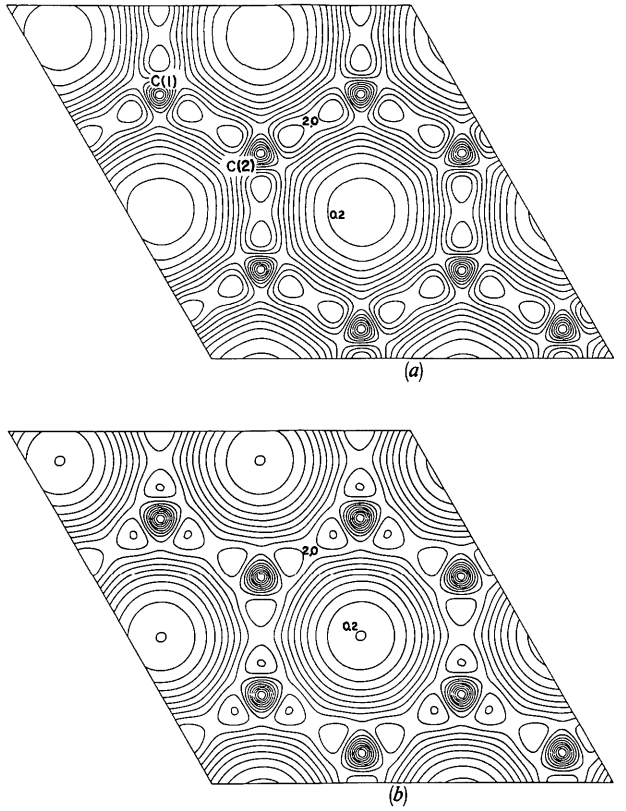

Fig. 2. Valence-charge density in the basal plane of graphite: (*a*) generated from the refinement parameters before extinction was included, (*b*) from parameters after extinction was included. The positions of atoms C(1) and C(2) are indicated in (*a*). Contours were drawn every 0·2 e Å^{-3}. Because the $1s^2$ core electron density has been omitted the contours at the C(1) and C(2) positions represent the 0·4 e Å^{-3} level. The estimated standard deviations of the populations for the charge terms indicate an error of ±0·1 e Å^{-3}.

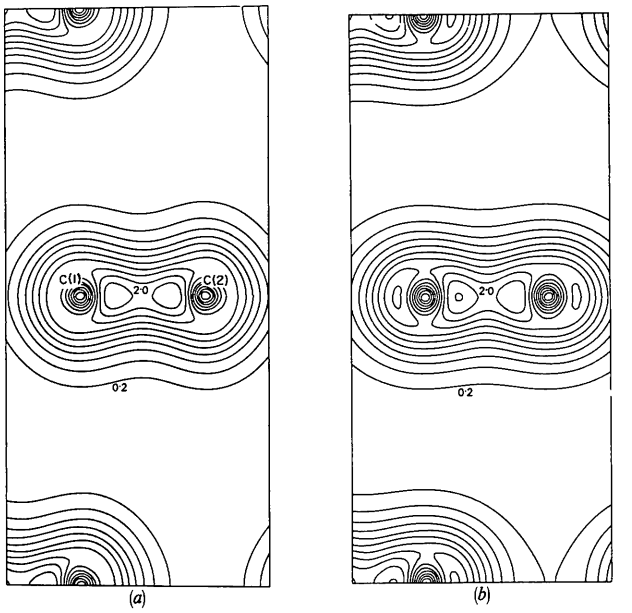

Fig. 3. Valence-charge density maps in a plane perpendicular to the basal plane of graphite and containing atoms C(1) and C(2): (*a*) generated from the refinement parameters before extinction was included, (*b*) from parameters after extinction was included. Contours are drawn every 0·2 e Å^{-3}. Because the $1s^2$ core electron density was not included, the level at the position of C(1) and C(2) is 0·4 e Å^{-3}. Atom C(1) is above and below equivalent atoms in adjoining layers, while C(2) is above and below the centers of hexagonal rings in adjacent layers.

When extinction corrections were made, the general features of the plots remained the same. The bonds contain somewhat less localized charge and there is a slight asymmetry in the bond. This asymmetry is approximately equal to the estimated error in the plots. From estimated standard deviations in the population coefficients, this error was estimated to be ±0·1 e Å^{-3}.

It is remarkable that atoms C(1) and C(2) are found to be very similar in the regions above and below the atoms; this is shown in Fig. 3 in the sections perpendicular to the basal plane. There is no structure in the interplanar region and no indication of bonding between C(1) and its neighbors above and below it. The covalent bonds are approximately symmetrical about the axis of the bond. The plot with extinction included, Fig. 3(*b*), accentuates the asymmetry mentioned above because of the particular section that is shown.

Discussion

The exponential term, α, in our refinement is essentially the same as that obtained for C atoms in diamond. The diamond study by Stewart (1973) yielded $\alpha = 3{\cdot}12 \pm 0{\cdot}06$ bohr^{-1} and the graphite refinement including extinction gave $3{\cdot}16 \pm 0{\cdot}05$ bohr^{-1}. These values are 8–10% less than the standard molecular value for C recom-

mended by Hehre, Stewart & Pople (1969).* Cromer, Larson & Stewart (1976) also found radial exponentials for C atoms in two organic molecules to be smaller than the standard molecular value.

The dominant deformation terms are the $P_{p,33}$ which are very efficient terms for building charge density between nearest neighbors in the basal plane. The signs of $P_{p,33}$ for C(1) and C(2) are such that charge is built up between atoms and subtracted in the opposite directions. $P_{p,20}$ and $P_{p,40}$ are of marginal significance. Positive signs of these deformations indicate charge build-up above and below the atom at the expense of charge in the basal plane. A negative sign reverses the effect.

The two $P_{p,00}$ populations should sum to eight electrons. Before the extinction refinement, the total valence-electron population was too low by four times the estimated standard deviation, σ, but the extinction correction brought the total valence electron population to within two times σ of what is necessary to maintain charge neutrality. This was one indication that the extinction refinement was able to distinguish between the large contribution of the 002 and 004 reflections to the extinction parameters and to the $P_{p,00}$ and α parameters.

The magnitude of graphite's thermal parameters makes this a low-temperature study. 50% of the motion perpendicular to the basal plane and 75% of the in-plane-motion is due to zero-point vibrations. The anisotropy of the thermal motion meant that correlations between thermal parameters and α_p, $P_{p,00}$, and scale were unusually low for charge-density refinements. The thermal parameters were not greatly affected by the various charge-density parameters that were added in the more general refinements. This is explained by the fact that the thermal parameters were sensitive to the high-order data, while the charge density parameters, as well as the extinction parameters, were sensitive to the intensities of low-order reflections. The thermal parameters in Table 2 are consistent with the neutron data of Trucano & Chen (1975) and have substantially lower estimated standard deviations.

The refinements fit the data to 14 parameters. With 99 independent reflections, an overdetermination of 7 to 1 existed. The radial functions have appreciable values for $\sin\theta/\lambda \leq 0{\cdot}7$ Å^{-1}. In this shell there are 35 independent reflections and this fact reduces the effective overdetermination, since the higher-order data are used to determine different parameters from the low-order data. Hamilton (1965) significance tests indicate the most general refinements significantly improved the fit to the data.

A further indication of errors involved in constructing the charge densities (in addition to the $\pm 0{\cdot}1$ e Å^3 derived from estimated standard deviations) can be obtained from a Fourier summation of the residuals. The values in a map formed with the half sphere of data varied from $-0{\cdot}3$ to $0{\cdot}5$ e Å^{-3}. This map had an irregular structure that was difficult to interpret, but the relatively high values compared with the errors estimated on the charge density maps are primarily due to the inclusion of the numerous high-order reflections with unit weight in the residual map. A map for the $\frac{1}{24}$ sphere of data contained maxima at high-symmetry positions, an effect discussed by Cruickshank & Rollett (1953).

There are several sources of error in the formal charge density map that were not included but which should be kept in mind: (1) no corrections for thermal diffuse scattering were made; (2) the simultaneous refinement of extinction and charge density depends on the ability of the formalism to separate out effects from a relatively small, critical part of the data set; (3) the assumption that the charge density associated with each atom varies with that atom must lead to some accommodation between thermal parameters and the charge-density parameters.

The authors wish to thank N. K. Hansen and P. Coppens for the prepublication use of their extinction refinement program. This work was supported by the National Science Foundation, Grant Nos. DMR76-21668 and CHE74-17592A03.

* The parameter α is twice the Slater-type atomic-orbital parameter ζ, since α describes electron densities.

References

BECKER, P. J. & COPPENS, P. (1975). *Acta Cryst.* A**31**, 417–425.

BERNAL, J. D. (1924). *Proc. Roy. Soc.* A**106**, 749–773.

BROWN, P. J. (1972). *Phil. Mag.* **26**, 1377–1394.

CROMER, D. T., LARSON, A. C. & STEWART, R. F. (1976). *J. Chem. Phys.* **65**, 336–349.

CRUICKSHANK, D. W. J. & ROLLETT, J. S. (1953). *Acta Cryst.* **6**, 705–707.

DONAHUE, J. (1975). *Nature, Lond.* **255**, 172.

ERGUN, S. (1973). *Nature Phys. Sci.* **241**, 65–67.

GOODMAN, P. (1976). *Acta Cryst.* A**32**, 793–798.

GÖTTLICHER, S. & WÖLFEL, Z. (1959). *Z. Elektrochem.* **63**, 891–901.

HAMILTON, W. C. (1965). *Acta Cryst.* **18**, 502–510.

HANSEN, N. K. & COPPENS, P. (1976). *Amer. Cryst. Assoc. Abstr.* **4**, 54.

HEHRE, W. J., STEWART, R. F. & POPLE, J. A. (1969). *J. Chem. Phys.* **51**, 2657–2664.

International Tables for X-ray Crystallography (1968). Vol. III. Birmingham: Kynoch Press.

International Tables for X-ray Crystallography (1974). Vol. IV. Birmingham: Kynoch Press.

LUKESH, J. S. (1950). *Phys. Rev.* **80**, 226–229.

PAULING, L. (1966). *Proc. Natl. Acad. Sci. US*, **56**, 1646–1652.

STEWART, R. F. (1973). *J. Chem. Phys.* **58**, 4430–4438.

STEWART, R. F. (1976). *Acta Cryst.* A**32**, 565–574.

STEWART, R. F. (1977). *Acta Cryst.* A**33**, 33–38.

TRUCANO, P. & CHEN, R. (1975). *Nature, Lond.* **258**, 136–137.